Contribution of Cooking Emissions to the Urban Volatile Organic Compounds in Las Vegas, NV

Matthew M. Coggon.[1*], Chelsea E. Stockwell.[1,2],Lu Xu[1,2,a], Jeff Peischl[1,2], Jessica B. Gilman[1], Aaron Lamplugh[1,2,b], Henry J. Bowman[3], Kenneth Aikin[1,2], Colin Harkins[1,2], Qindan Zhu[1,2,c], Rebecca H. Schwantes[1], Jian He[1,2], Meng Li[1,2], Karl Seltzer[4], Brian McDonald[1], Carsten Warneke[1]

[1] NOAA Chemical Sciences Laboratory (NOAA CSL), Boulder, CO, USA
[2] Cooperative Institute for Research in Environmental Sciences, University of Colorado Boulder, Boulder, CO, USA
[3] Department of Physics and Astronomy, Carleton College, Northfield, MN, USA
[4] U.S. Environmental Protection Agency, Triangle Park, NC, USA
[a] now at Department of Energy, Environmental and Chemical Engineering, Washington University in St. Louis, Missouri, USA
[b] now at Institute of Behavioral Science, University of Colorado, Boulder, CO, USA
[c] now at Department of Earth, Atmospheric and Planetary Sciences, Massachusetts Institute of Technology, Cambridge, MA, USA

*corresponding author: matthew.m.coggon@noaa.gov

Abstract

Cooking is a source volatile organic compounds (VOCs) that degrades air quality. Cooking VOCs have been investigated in laboratory and indoor studies, but the contribution of cooking to the spatial and temporal variability of urban VOCs is uncertain. In this study, a proton-transfer-reaction time-of-flight mass spectrometer (PTR-ToF-MS) is used to identify and quantify cooking emission in Las Vegas, NV with supplemental data from Los Angeles, CA and Boulder, CO. Mobile laboratory data show that long-chain aldehydes, such as octanal and nonanal, are significantly enhanced in restaurant plumes and regionally enhanced in areas of Las Vegas with high restaurant density. Correlation analyses show that long-chain fatty acids are also associated with cooking emissions and the relative VOC enhancements observed in regions with dense restaurant activity are very similar to the distribution of VOCs observed in laboratory cooking studies. Positive matrix factorization (PMF) is used to quantify cooking emissions from ground site measurements and compare the magnitude of cooking to other important urban sources, such as volatile chemical products and fossil fuel emissions. PMF shows that cooking may account for as much as 20% of the total anthropogenic VOC emissions observed by PTR-ToF-MS. In contrast, emissions estimated from county-level inventories report that cooking accounts for less than 1% of urban VOCs. Current emissions inventories do not fully account for the emission rates of long-

chain aldehydes reported here and further work is likely needed to improve model representations of important aldehyde sources, such as commercial and residential cooking.

1. Introduction

Volatile organic compounds (VOCs) degrade air quality and are emitted to urban air from many sources, including fossil fuel combustion (Warneke et al., 2012), the use of volatile chemical products (VCPs, McDonald et al., 2018), industrial processes (Zhang et al., 2004), residential heating and wood burning (e.g., McDonald et al., 2000; Coggon et al., 2016), cooking (Wernis et al., 2022), and urban vegetation (e.g., Churkina et al., 2017). Each source emits a diverse set of molecules that react alongside nitrogen oxides ($NO + NO_2 = NO_x$) to form ozone. Recent field work in major US metropolitan areas has characterized the distribution of urban VOCs to assess the chemical fingerprint of understudied emission sources, such as VCPs (Gkatzelis et al., 2021b; Peng et al., 2022). These studies have shown that these sources emit oxygenated VOCs (oVOCs) which react to form ozone and secondary organic aerosol. Models have been updated to better describe the emissions and chemistry of select oVOCs, including alcohols, siloxanes, glycols, and furanoids (Coggon et al., 2021; Pye et al., 2023; Qin et al., 2021).

Many oVOCs are emitted to urban air that have not been well-studied or incorporated into air quality models (Karl et al., 2018). For example, McDonald et al. (2018) showed that $C > 5$ aldehydes measured in Los Angeles, CA could not be explained by emissions inventories that contain VCPs, fossil fuels, or biogenic sources. Cooking is a source of oVOCs that is rich in aldehydes and fatty acids (Klein et al., 2016a). Cooking VOCs have been extensively characterized in the laboratory (Bastos and Pereira, 2010; Klein et al., 2016a; Klein et al., 2016b; Schauer et al., 1999; Zhao and Zhao, 2018) and it has been shown that cooking is a key activity controlling the budget of VOCs measured in indoor air (Arata et al., 2021; Klein et al., 2019; Klein et al., 2016a). Numerous studies have shown that cooking is a ubiquitous and important component of organic aerosol in urban areas (Hayes et al., 2013; Robinson et al., 2006; Robinson et al., 2018; Shah et al., 2018; Slowik et al., 2010; Zhang et al., 2019) yet only a few studies have been conducted to characterize cooking VOCs in ambient datasets (e.g., Peng et al., 2022; Wernis et al., 2022).

Cooking emissions result from the combustion and high temperature decomposition of food and oils (Bastos and Pereira, 2010; Umano and Shibamoto, 1987). During heating, fatty acids undergo thermal oxidation to produce emissions of aldehydes, ketones, alcohols, acids, and other products of depolymerization (Bastos and Pereira, 2010; Schauer et al., 1999). The use of spices emits monoterpenes and their derivatives (Klein et al., 2016a). Studies that have speciated VOCs from a variety of Western cooking styles (e.g., charbroiling, grilling, frying) and ingredients (e.g., oils, meats, and vegetables) show that aliphatic C_1-C_{11} aldehydes account for a large fraction of VOCs measured by gas-chromatography and mass spectrometry (e.g., Bastos and Pereira, 2010; Klein et al., 2016b; Peng et al., 2017; Schauer et al., 1999). For example, Klein et al. (2016b)

reported that aldehydes represent > 60% of the VOC mass emitted from frying or charbroiling meats and vegetables.

Ambient observations have shown that long-chain aldehydes are present in urban air at significant mixing ratios (e.g., nonanal ~ 100 – 200 ppt, Bowman et al., 2003; Wernis et al., 2022). Recent studies have used hexanal and nonanal as markers for cooking emissions in in Atlanta, GA and Livermore, CA (Peng et al., 2022; Wernis et al., 2022). These species correlated with morning and evening meal preparation, and it was suspected that restaurant emissions were a driving factor for the observed temporal variability in Livermore (Wernis et al., 2022). In addition to cooking, certain long-chain aldehydes are known to be emitted from diesel exhaust (e.g., hexanal, Gentner et al., 2013), and some are produced from the emission and ozonolysis of oils and fatty acids present in human skin, at the surface of ocean waters, or from other surfaces that contain unsaturated lipids (Kruza et al., 2017; Liu et al., 2021; Wang et al., 2022; Kilgour et al., 2021).

The high abundance of aliphatic aldehydes from cooking suggests that they may be useful markers to constrain cooking VOC emissions in urban areas. The utility of aldehydes as cooking markers relies on the characterization of their sources in the atmosphere as well as careful characterization of measurement techniques used to detect these species. Short-chain aldehydes ($C< 5$) are unlikely to serve as useful markers because they are produced in the atmosphere from the OH oxidation of primary organic molecules and are also directly emitted from fossil fuel emissions and biomass burning (Gentner et al., 2013; Koss et al., 2018; de Gouw et al., 2018). Long-chain aliphatic aldehydes ($C > 6$) have the potential to be useful markers for cooking in urban areas, but their primary sources, spatial distributions, and abundances in the atmosphere remain uncertain. Some long-chain aldehydes may be emitted from mobile sources (e.g.,Gentner et al., 2013) while others may be emitted from surface ozone chemistry (e.g., Liu et al., 2021). No field measurements have reported the spatial distribution of long-chain aldehydes to determine likely sources in urban air.

This study evaluates the contribution of commercial and residential cooking emissions to urban VOCs using mobile laboratory and ground site observations made in Las Vegas, NV with supplemental observations made Los Angeles, CA and Boulder, CO. Mobile laboratory measurements show that long-chain aliphatic aldehydes are significantly enhanced downwind of restaurants and exhibit spatial distributions in urban regions of Las Vegas that closely matches restaurant density. Furthermore, these measurements show that the distribution of VOCs that correlate with long-chain aldehydes strongly resembles the distribution observed in restaurant plumes. We conduct a source apportionment analysis to determine the extent to which cooking emissions impact urban VOCs relative to other important anthropogenic sources, such as motor vehicles and VCPs, and compare these observations to commonly used emissions inventories.

2. Methods

2.1. Field Campaign Description: SUNVEx

Air quality measurements were performed during the 2021 Southwest Urban NO_x and VOC Experiment (SUNVEx) in Las Vegas, NV. Las Vegas is a major resort city in the Southwest US that is known for its entertainment industry, gambling, dining, and nightlife. During SUNVEx, trace gases including VOCs, nitrogen oxides ($NO_x = NO + NO_2$), and carbon monoxide (CO) were measured from 30 June– 27 July, 2021 at a ground site located at the Jerome Mack Air Quality Station (Fig. 1). Mobile measurements were also conducted using the NOAA mobile laboratory to characterize the spatial distribution of anthropogenic and biogenic emissions.

Figure 1 is a map of the Las Vegas valley showing residential, commercial, and entertainment districts. The blue dots show the locations of restaurants that are cataloged in health inspection reports maintained by the Southern Nevada Health District (SNHD, 2021). These reports include data for restaurants, bars, and other locations that provide food or beverages. The data presented here have been screened to only include locations categorized as restaurants that have been inspected within one year of the SUNVEx campaign. Further details about the dataset is provided in the Supplemental Information. The wind rose in Fig. 1 is centered at the Jerome Mack Air Quality Station and highlights the prevailing wind directions and speeds observed at the ground site. The Las Vegas region is impacted by significant emissions from the Las Vegas Strip (the purple shaded region in the center of Fig. 1), which is an entertainment district with a high density of casinos, hotels, bars, and restaurants that emit VCP, fossil fuel, and cooking VOCs. The Jerome Mack ground site is located ~8km east of the Las Vegas Strip in a residential area with restaurants and small commercial businesses located along major streets. The prevailing wind patterns show that ground measurements were routinely impacted by air transported from the Las Vegas Strip along with regions to the north with higher commercial activity.

The mobile laboratory sampled air in regions across Las Vegas to investigate anthropogenic emissions from residential, commercial, and entertainment districts (Fig 1). A full description of the mobile laboratory is provided by Eilerman et al. (2016) Briefly, instruments sampled air from inlets located on the roof towards the front of the vehicle. Data were analyzed when the mobile laboratory was in motion in order to eliminate periods when instruments may have self-sampled exhaust. When operating as a ground site or during stationary sampling, the mobile laboratory engine was turned off and instruments were powered by batteries charged with a MagnaSine inverter/charger (MS2812). Pressure, temperature, relative humidity, and wind speed / direction were monitored by a suite of meteorological sensors (Airmar 200 WX, R.M. Young 85004 sonic anemometer). Mobile laboratory position, speed, and heading were measured by a differential GPS (ComNav G2B).

Seven mobile laboratory drives were conducted between 27 June and 31 July, 2021. Supplemental Figure S1 shows the individual drive paths on each day. Drives times ranged between 4 – 10 hr long and the cumulation of the sampling paths provided a nearly-complete survey of the Las Vegas Valley and surrounding desert ecosystem (Fig. 1). Most drives included focused sampling along Las Vegas Strip due to its significant influence on the spatial distribution of VOCs in the Las Vegas Valley. The Las Vegas Strip was sampled at different times of day (afternoon: 12:00 – 18:00 PM, evening: 18:00 – 22:00 PM, night: 22:00 PM – 02:00 AM) to investigate changes to anthropogenic VOC mixing ratios as a result of increased dining, gambling, and entertainment activities in the evening.

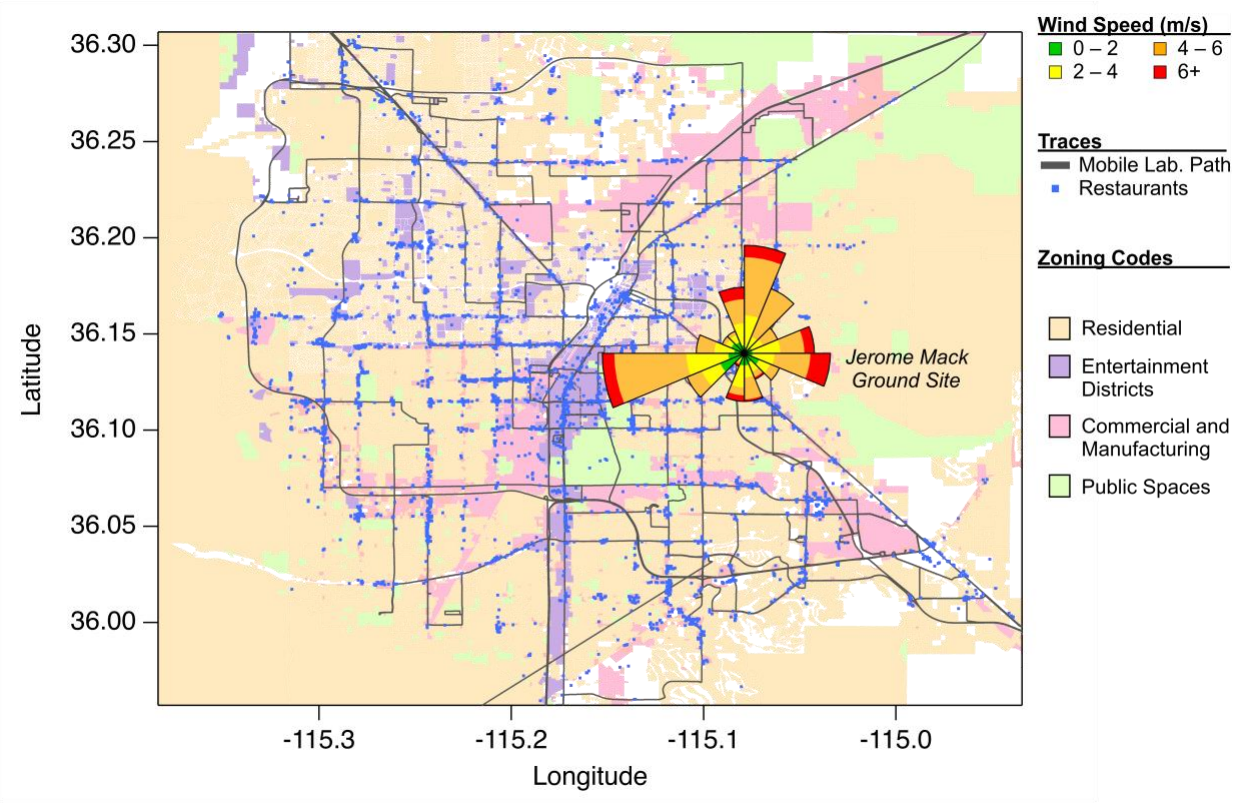

Figure 1: Zoning map of the Las Vegas region showing regions sampled by the mobile laboratory. Zoning data are available from the Clark County GIS Management Office (https://clarkcountygis-ccgismo.hub.arcgis.com, accessed September 2023) The blue dots show the locations of restaurants in the Las Vegas valley that are cataloged in health inspection reports maintained by the Southern Nevada Health District (SNHD, 2021). The wind rose shows the prevailing wind directions and speed observed at the Jerome Mack ground site. The wind rose is centered on the map at the location of Jerome Mack.

2.2. Field Campaign Description: RECAP-CA and Supplemental Mobile Drives

Additional VOC measurements were conducted in the Los Angeles basin during the Re-Evaluating the Chemistry of Air Pollutants in California (RECAP-CA) study. These measurements

serve as a comparison to the observations in Las Vegas. Ground measurements during RECAP-CA were performed at the California Institute of Technology in Pasadena, CA from 1 August – 5 September, 2021. VOCs and other trace gases were sampled from the top of a 10 m tower. The location of the ground site was located within 0.5km from the ground site used during the 2010 CalNex campaign (Ryerson et al., 2013). The Pasadena ground site has been previously characterized and is a downwind receptor site for air impacted by emissions from downtown Los Angeles, CA (e.g., de Gouw et al., 2018).

Supplemental mobile laboratory measurements were performed in Los Angeles, CA and Boulder, CO to sample VOCs downwind of individual restaurants. These measurements serve as comparisons against the restaurant emissions observed in the Las Vegas region.

2.3. Instrument Descriptions

PTR-ToF-MS

VOC mixing ratios were measured using a Vocus proton-transfer-reaction time-of-flight mass spectrometer (PTR-ToF-MS) (Yuan et al., 2016; Krechmer et al., 2018). The PTR-ToF-MS measures a large range of aromatics, alkenes, nitrogen-containing species, and oxygenated VOCs. A full description of the instrument during SUNVEx is provided by Coggon et al. (2024). Briefly, the PTR-ToF-MS sampled air a ~2 L min^{-1} through a short (< 1m) inlet while in the mobile laboratory. At the ground sites, the instrument sampled at ~20 L min^{-1} from a 10 m tower. The Vocus drift tube was operated at 110°C with an electrical field (E) to number density (N) ratio (E/N) of 140 Td. Instrument backgrounds were determined every 2 h for ground site experiments and every ~15-30 minutes during drives by passing air through a platinum catalyst heated to 350°C. Data were processed following the recommendations of Stark et al. (2015) using the Tofware package in Igor Pro (WaveMetrics). The PTR-ToF-MS was calibrated using gravimetrically-prepared gas standards for typical VOCs such as acetone, methyl ethyl ketone, toluene, and C8-aromatics. Many compounds unavailable in gas standards were quantified by liquid calibration methods as described by Coggon et al. (2018). This included D5-siloxane, parachlorobenzotriflouride, octanal and nonanal. All other compounds were quantified using estimated proton-transfer-reaction rate constants as described by Sekimoto et al. (2017). Further corrections were applied to masses assigned to long-chain aldehydes based on observed mass-dependent changes in fragmentation patterns described in the Supplemental Information and shown in Fig. S4.

GC-PTR-ToF-MS

PTR-ToF-MS only resolves VOC molecular formula. To identify structural isomers, a custom-built gas-chromatography (GC) instrument was used to collect and pre-separate VOCs

prior to detection by PTR-ToF-MS. A full description of the system is provided by Stockwell et al. (2021) and its operation during SUNVEx is described by Coggon et al. (2024). Briefly, the GC consists of a DB-624 column (Agilent Technologies, 30 m, 0.25 mm ID, 1.4 μm film thickness) and oven identical to the system described by Lerner et al. (2017). VOCs were condensed onto a liquid nitrogen cryotrap, flash vaporized, then passed through the column using nitrogen as a carrier gas. The column was linearly heated during separation from 40-150°C. The effluent from the column was directly injected in the PTR-ToF-MS inlet. At the Jerome Mack ground site, GC samples were collected every 2 hours and immediately analyzed by PTR-ToF-MS. GC samples were also collected during a nighttime mobile laboratory drive on July 31, 2021. These samples were used to help interpret PTR-ToF-MS measurements along the Las Vegas Strip.

A key goal of this study is to characterize the spatial and temporal pattern of long-chain aldehydes. Aldehydes and ketone isomers are quantified by PTR-ToF-MS using measurements of the proton-transfer product ions (= VOC mass + H^+). Aliphatic aldehydes also undergo dehydration (= VOC mass + H^+ – H_2O) and fragmentation reactions, which effectively lowers the instrument sensitivity to the proton-transfer product. Consequently, it can be challenging to unambiguously assign carbonyl ions to specific isomers. In the Supplemental Information, GC-PTR-ToF-MS and mobile laboratory PTR-ToF-MS measurements show that C_8 and C_9 carbonyls measured in urban areas are predominantly associated with octanal (detected at m/z 129, $C_8H_{16}OH^+$) and nonanal (detected at m/z 143, $C_9H_{18}OH^+$). These ions have no detectable interferences from ketone isomers in GC-PTR-ToF-MS spectra (Fig. S3) and the ratio of these ions with carbonyl dehydration products most closely matches the fragmentation patterns of aldehydes (Fig. S5). Smaller carbonyls have significant interferences from ketone isomers, which complicates their use as markers for aldehyde emissions. Here, we focus on the spatial and temporal trends of octanal and nonanal and use these markers to determine the fingerprint of cooking VOC emissions. We note that mixing ratios of nonanal and octanal are quantified based on the signal at the proton-transfer product and not from the sum of all fragments. The fragmentation products from octanal, nonanal, and other aldehydes overlap with signals from cycloalkanes emitted from fossil fuels and biogenic isoprene (Coggon et al., 2024; Gueneron et al., 2015).

LGR Carbon Monoxide

Carbon monoxide was measured at the Las Vegas ground site using off-axis integrated cavity output spectroscopy (ABB Inc./Los Gatos Research model F-N_2O/CO-23r) (Roberts et al., 2022). Data were measured at 1-Hz and reported as 1-minute averages. Instrument precision was estimated to be ±0.2 ppb (1-σ), and the 1-σ uncertainty was estimated to be ±1% based on calibrations in the laboratory before and after the SUNVEx/RECAP-CA projects.

2.4. Positive Matrix Factorization

Positive matrix factorization (PMF) is used to analyze the PTR-ToF-MS data and apportion VOCs to cooking and other urban sources in Las Vegas. PMF was conducted using the Source Finder (SoFi) software package in Igor Pro (Canonaco et al., 2013). Two periods are analyzed when PTR-ToF-MS measurements were available : 30 June–9 July and 19–27 July. In this analysis, we constrain PMF with a mobile source profile derived from mobile measurements following the recommendations of Gkatzelis et al. (2021b). We present a solution of factors representing mobile sources, VCPs, cooking, and regional chemical oxidation. A full description of the PMF analysis is provided in the Supplemental Information.

3. Results

3.1. Long-chain aldehydes downwind of restaurants

Previous studies have shown that cooking organic aerosols (COA) from dense restaurant clusters exhibit plume-like behavior that can impact local air quality at spatial scales of 0.5–1 km (Robinson et al., 2018; Shah et al., 2018). For example, Robinson et al. (2018) showed that organic aerosol was enhanced by as much as 100–200 μg m^{-3} within 1 km of restaurants and resulted in average local organic aerosol enhancements of 3.2 μg m^{-3}. Consequently, it is expected that cooking VOCs would also be significantly enhanced in close proximity of restaurants or in regions with significant restaurant activity.

Figure 2 shows mobile laboratory measurements of nonanal and octanal mixing ratios downwind of two fast food restaurants in Los Angeles, CA and Boulder, CO. Mixing ratios of markers typically representative of personal care products (D5-siloxane) and motor vehicle emissions (benzene) are also shown to highlight the presence of other sources in the region. The restaurant in Los Angeles primarily serves hot dogs, while the restaurant in Boulder serves hamburgers and fried foods. The highlighted boxes show periods where the mobile laboratory was parked to sample restaurant emissions. All other data reflect sampling periods when the mobile laboratory was driven through densely populated areas of Los Angeles and Boulder. In both cases, the mobile laboratory was parked within 50m of the restaurant exhausts.

Aldehyde mixing ratios downwind of both restaurants exceeded 1 ppb. Generally, these mixing ratios were elevated relative to the surrounding densely populated regions. Octanal and nonanal mixing ratios were not correlated to benzene or other molecules primarily emitted from motor vehicles (Fig. 2). These results suggest that octanal and nonanal are not significantly enhanced in tailpipe emissions in these regions, which is consistent with previous studies showing that on-road emission factors of C_8 – C_9 aldehydes from US vehicles are low (Gentner et al., 2013). Octanal and nonanal were not strongly correlated with mixing ratios of D5-siloxane, though there were periods when long-chain aldehyde and D5-siloxane enhancements were coincident. This may

result from the co-location of food and people or a possible human emission source. Octanal and nonanal are known to be produced from skin ozonolysis (Liu et al., 2021; Wang et al., 2022) and carbonyls are potential ingredients in fragranced consumer products, though emissions inventories and measurements of fragrance formulations do not indicate that octanal and nonanal are significant ingredients of VCPs (Hurley et al., 2021; McDonald et al., 2018; Yeoman et al., 2020).

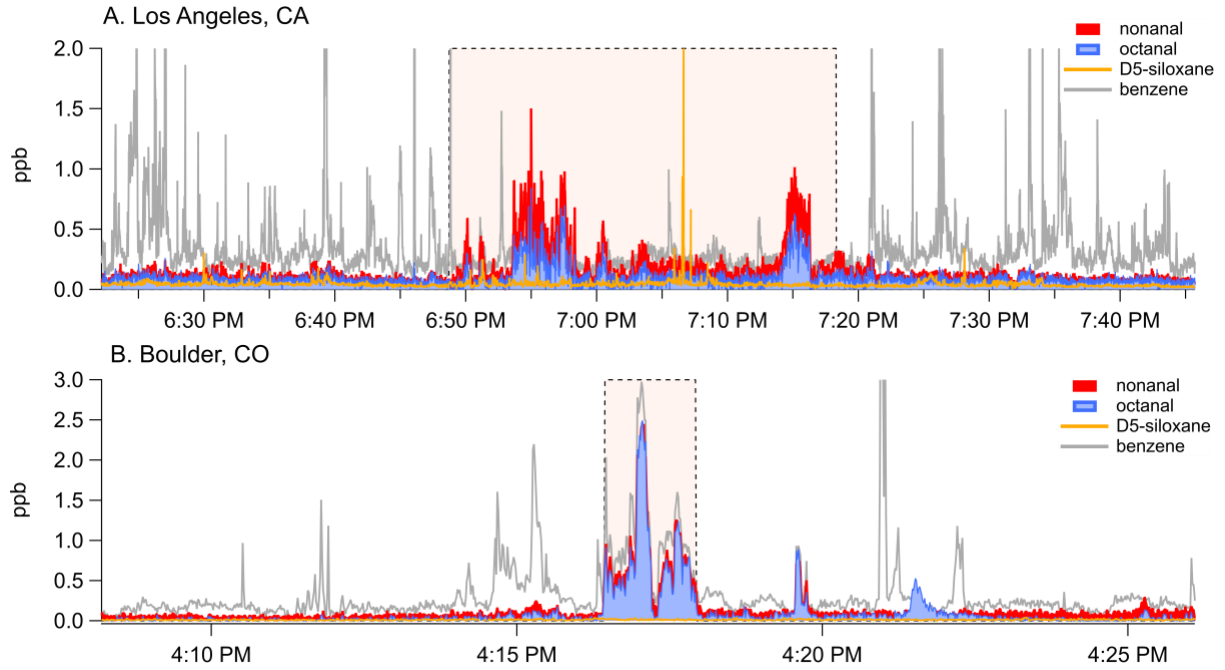

Figure 2: Mobile laboratory measurements of octanal, nonanal, D5-siloxane, and benzene in (A) Los Angeles, CA and (B) Boulder, CO. The shaded regions show periods when the mobile laboratory was parked downwind of a restaurant that primarily serves hot dogs (Los Angeles) and a restaurant that primarily serves hamburgers (Boulder). All other data were collected while the mobile laboratory sampled air in populated areas.

Figure 2 shows that restaurants are a strong source of aliphatic aldehydes, such as octanal and nonanal. Based on these enhancements, it is likely that VOCs emitted from cooking are significantly enhanced in regions with dense restaurant activity. These inferences are consistent with previous mobile laboratory observations of primary organic aerosols. For example, Robinson et al. (2018) found that organic aerosol in commercial districts of Pittsburgh, PA with significant restaurant density was nearly twice as concentrated as organic aerosol in areas with highways and significant traffic. Similar results were observed by Shah et al. (2018) in Oakland, CA where COA constituted ~ 50% of the primary organic aerosol and was observed to be enhanced in downtown regions where restaurant density was highest. Both studies demonstrate that air quality in urban areas is significantly impacted by restaurant density.

Las Vegas is a sprawling city where most emission sources are concentrated along the Las Vegas Strip (Figure 1). Figure 3 shows the spatial distribution of octanal and nonanal from all of the mobile laboratory drives, along with a map of restaurant density calculated using the restaurant location data shown in Figure 1. Each pixel is determined by summing the number of restaurants over a 0.5 x 0.5 km grid. Figure 3 shows that octanal and nonanal are well-correlated ($R^2 = 0.82$) and predominantly enhanced in the Las Vegas Strip area where anthropogenic emissions are the highest. Figure 3A shows that this region has a high restaurant density compared to other regions of the Las Vegas Valley. We note that brief (~1s), isolated enhancements in PTR-ToF-MS measurements of octanal are observed outside of the Las Vegas Strip. These enhancements also have corresponding increases in nonanal, though the ratios of these species are different than what is observed along the Las Vegas Strip.

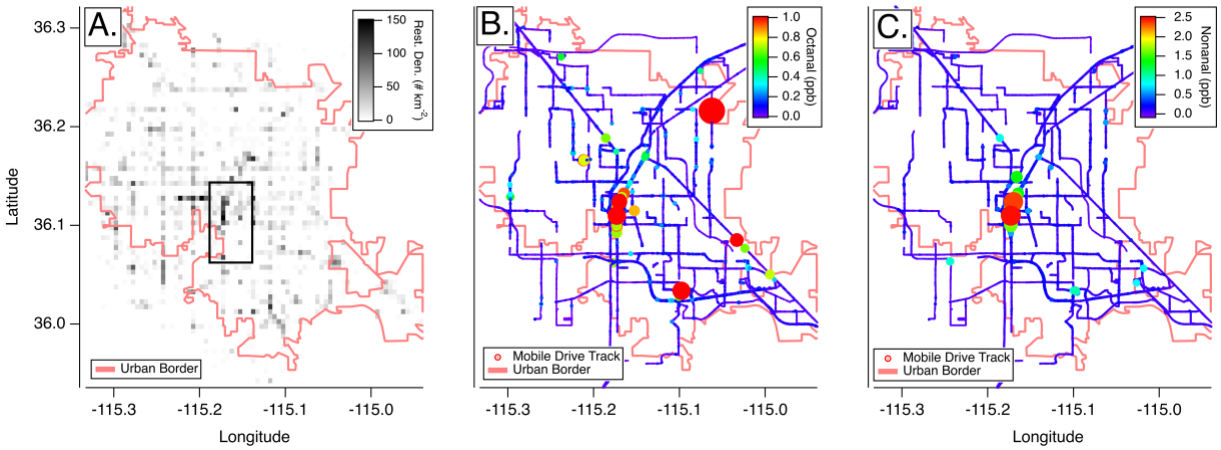

Figure 3: (A) Restaurant density in Clark County, NV. Restaurant density is determined using the restaurant locations shown in Fig. 1 and is calculated by summing the number of restaurants located within a 0.5 x 0.5 km grid. The rectangle shows the approximate region of the Las Vegas Strip. Panels (B) and (C) show the mobile laboratory path colored by octanal and nonanal mixing ratios, respectively. Markers are sized by the corresponding mixing ratios shown in the color scales.

Figure 4 further evaluates the spatial distribution of long-chain aldehydes by comparing nonanal mixing ratios against the restaurant density in the proximity of the mobile laboratory. Here, restaurant density is extracted from Fig. 3A by selecting the grid cells that are coincident with the mobile laboratory position while sampling in the vicinity of the Las Vegas Strip (indicated by the black box shown in Fig. 3A). The three drives shown correspond to mid-day (12:00 – 7:00 PM local time), evening (8:00 – 11:00 PM), and late-night (9:30 PM – 1:00 AM) sampling. The drives show that nonanal is generally enhanced in regions with higher restaurant density. Nonanal mixing ratios are high and sustained along the Las Vegas Strip during the evening drive when activities from the entertainment industry, including dining, are likely most frequent (panel B). Enhancements in nonanal are also observed during the mid-day and late-night drives (panel A + C), though mixing ratios appear more variable. Octanal exhibits a similar relationship with

restaurant density. These results are consistent with the observed enhancements in organic aerosol seen previously observed in dense restaurant regions (Robinson et al., 2018; Shah et al., 2018).

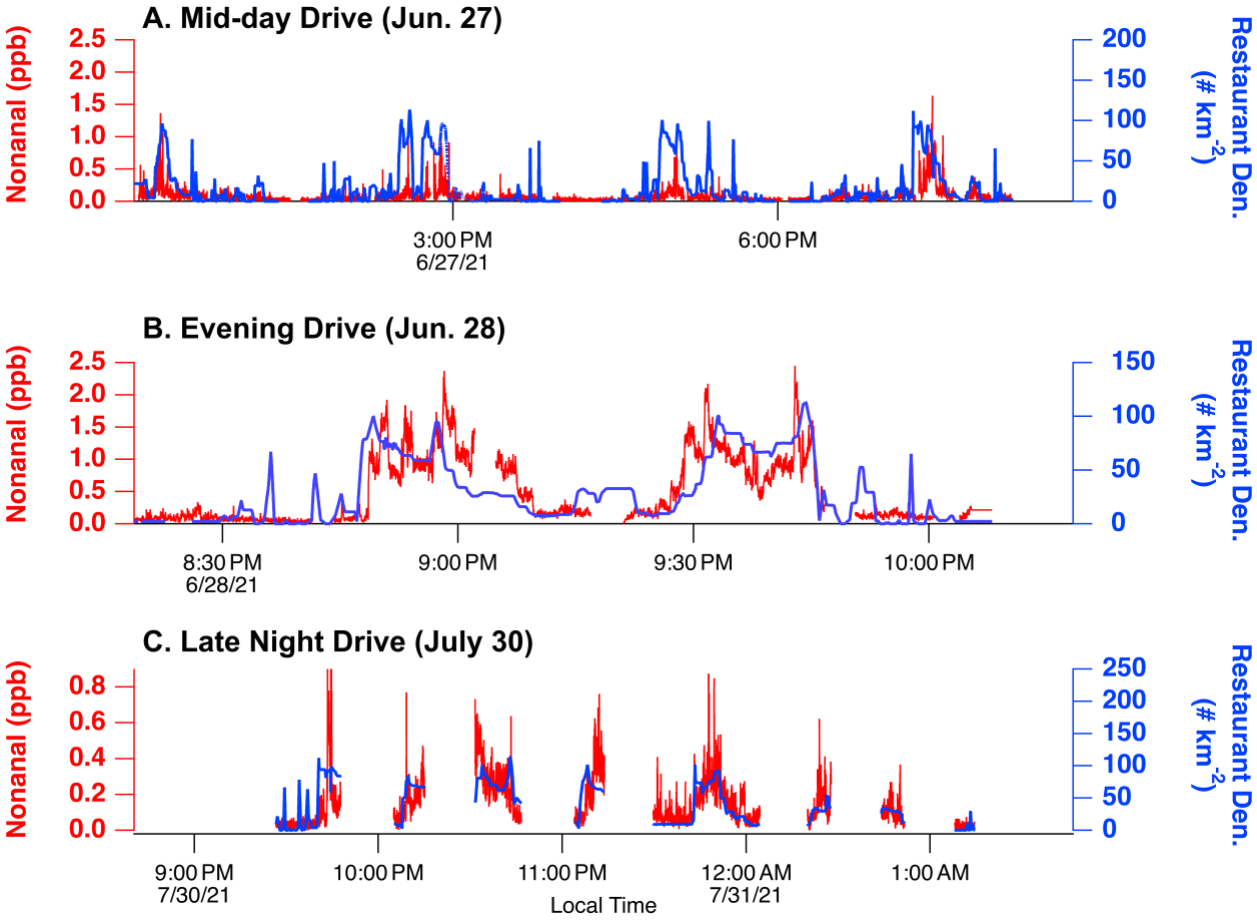

Figure 4: Nonanal mixing ratios and corresponding restaurant density in areas sampled by the mobile laboratory. Restaurant density is determined by averaging restaurant data in Figure 3A on a 0.5 km x 0.5 km grid, then extracting data along the mobile laboratory drive track.

Figure S2 shows that the octanal and nonanal observed along the Las Vegas Strip are also measured at the Jerome Mack ground site. The two species are well-correlated ($R^2 > 0.86$) and most abundant at night, likely due to a combination of meteorology (i.e., shallow nocturnal boundary layer) and higher emissions in the evening (e.g., Fig. 4). Figure S2 also shows octanal and nonanal mixing ratios observed at the Caltech ground site in Pasadena, CA. These measurements exhibit similar temporal behavior and demonstrate that long-chain aldehyde are ubiquitous in many urban regions. We note that nonanal ratios reported here are similar to those observed from previous studies (~ 100 – 200 ppt, Bowman et al., 2003; Wernis et al., 2022).

3.2. Species co-emitted with octanal and nonanal in the Las Vegas Strip

Octanal and nonanal represent a significant fraction of cooking VOCs measured in laboratory studies (>5%) but are just two of many VOCs emitted from cooking activities (Klein et al., 2016b). To assess the potential fingerprint of VOCs in regions impacted by commercial cooking, we evaluate the VOC mass spectra from the Las Vegas Strip and identify cooking VOCs by correlating PTR-ToF-MS ions to observations of nonanal. Species are only included in this analysis if the detected ion likely represents a proton-transfer product (i.e., fragments are excluded) and correlates with nonanal with $R^2 > 0.8$. This high correlation coefficient is used to identify potential co-emitted species, while excluding VOCs emitted from sources that are co-located with restaurants in the Las Vegas Strip, such as mobile sources and VCPs. For example, D5-siloxane correlates with nonanal with an R^2 of 0.78. Personal care product emissions are significant along the Las Vegas Strip (D5-siloxane mixing ratios > 1 ppb on June 28, 2021), but octanal and nonanal have not been reported as major components of fragranced personal care products (e.g., McDonald et al., 2018; Steinemann, 2015; Steinemann et al., 2011; Yeoman et al., 2020; Hurley et al., 2021). A high correlation is expected because food and people are co-located; however, in this analysis D5-siloxane and compounds with $R^2 < 0.8$ are excluded.

Figure 5 shows the correlation spectrum of the VOCs to nonanal. The correlation coefficient and the ratio of VOCs to nonanal are plotted versus the detected mass. The compounds that correlate with nonanal have chemical formula of either C_xH_yO or $C_xH_yO_2$ with carbon numbers ranging between C_2 – C_{11}. Compounds with formula C_xH_yO are likely aliphatic aldehydes with varying degrees of saturation and some key species are highlighted for each carbon grouping (Figure 6A). Species with the highest correlation to nonanal include octenal ($R^2 = 0.94$), decenal ($R^2 = 0.93$), butenal/crotonaldehyde ($R^2 = 0.93$), and acrolein ($R^2 = 0.92$). While individual C_3 – C_5 species are the largest contributors to the total signal, the sum of long-chain aldehydes (C_6 – C_{11}) are >50% of the total spectrum.

Compounds with formula $C_xH_yO_2$ likely correspond to fatty acids (Figure 5B). Gaseous acids are released from the high temperature decomposition of long-chain acids present in meat and previous studies have measured significant emissions of heptanoic, octanoic, nonanoic, and decanoic acid (Schauer et al., 1999; Klein et al., 2016b). The acids in Figure 5B are some of the most abundant acids observed along the Las Vegas Strip. The strong correlation of nonanal to fatty acids further supports that cooking emissions are an important emitter of long-chain aldehydes in this region.

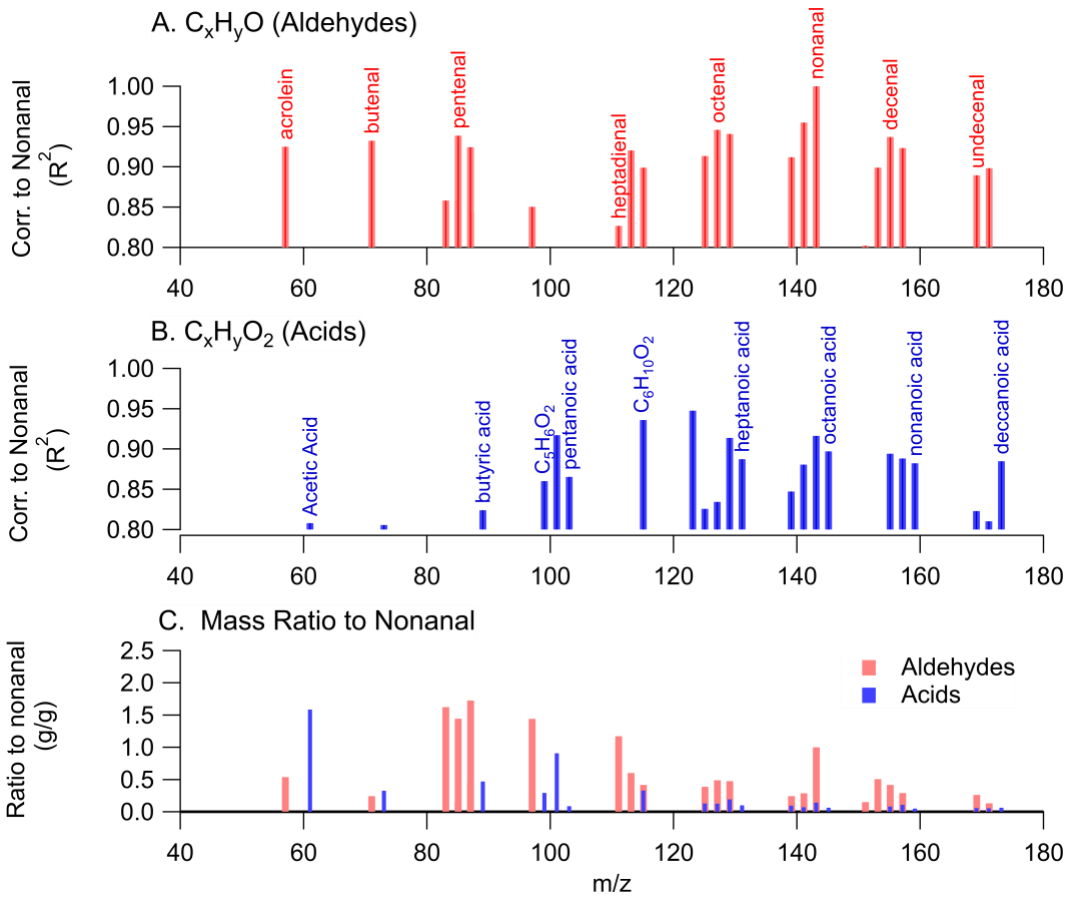

Figure 5: VOC correlation to nonanal in downtown Las Vegas during nighttime mobile sampling for (A) C_xH_yO species (assigned as aldehydes) and (B) $C_xH_yO_2$ species (assigned as acids). (C) VOC / nonanal ratios for species that correlate with nonanal with $R^2 > 0.8$.

Figure 6 compares the spectra measured along the Las Vegas Strip to the spectra derived from the individual restaurants sampled in Boulder, CO and Los Angeles, CA (Figure 2). The VOC ratios observed in the restaurant plumes are strikingly similar to the ratios observed in downtown Las Vegas, which further supports that the aldehydes and acids measured along the Las Vegas Strip were associated with restaurant emissions. The spectra are also comparable to available PTR-ToF-MS spectra of meat cooking emissions reported by Klein et al. (2016b). These laboratory measurements show that heptadienal, octanal, nonanal, decadienal, and undecanal are key $C_7 - C_{11}$ aldehydes emitted when cooking meats with vegetable oils. The same aldehydes are observed in the Las Vegas Strip area.

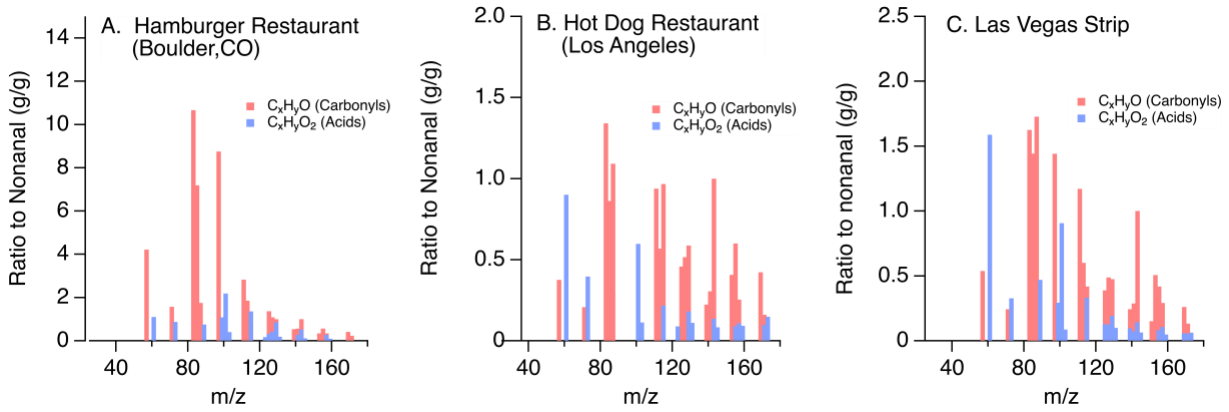

Figure 6. Comparison of (A) restaurant emissions from a hamburger restaurant in Boulder, CO, (B) restaurant emissions from a hot dog restaurant in Los Angeles, and (C) cooking emissions from measurements along the Las Vegas Strip.

Klein et al. (2016b) speciated laboratory cooking emissions and distinguished emissions of higher carbon aldehydes (C ≥ 7) and acids from lower carbon species. These groupings are also distinct in the laboratory VOC distributions reported by Schauer et al. (1999) and are suspected to be signatures of cooking emissions in Las Vegas (e.g., Fig. 5). Figure 7 compares the distribution of C ≥ 7 oxygenates observed in this study (top row) with the distributions reported by laboratory studies (bottom row). Schauer et al. (1999) observed that ~10% of the C ≥ 7 mass emitted from beef charbroiling was attributed to acids, while 90% was attributable to carbonyls largely composed of aldehydes. Klein et al. (2016b) observed a similar profile averaged across a range of experiments using meats and vegetable oils. In the Las Vegas Strip area, acids represented ~16% of mass associated with C ≥ 7 compounds, while the remainder is associated with carbonyls dominated by aldehydes. Carbonyls are the dominant C ≥ 7 emissions from both restaurants sampled by the mobile laboratory. The similarity in the distributions between laboratory and field observations further suggest that long-chain aldehydes are useful markers for constraining cooking emissions in urban air.

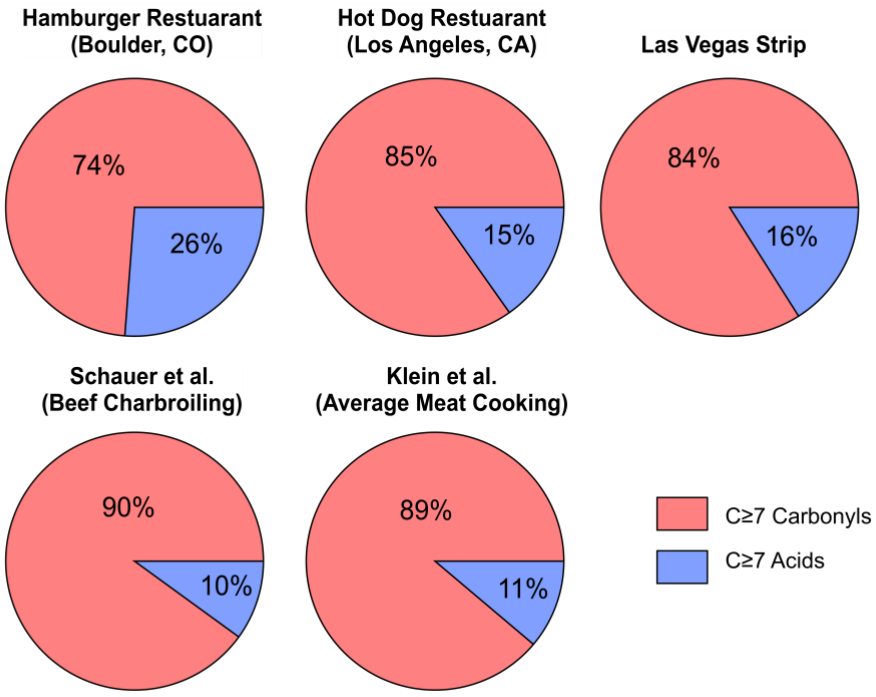

Figure 7: Comparison of the C ≥ 7 oxygenates measured as part of this study (top row) with those observed from laboratory experiments reported by Schauer et al. (1999) and Klein et al. (2016b) (bottom row). The distribution from Schauer et al. (1999) reflects emissions from beef charbroiling, while the distribution from Klein et al. (2016b) is derived as the average distribution from the frying of pork, chicken, beef, and fish in a range of vegetable oils.

4. Source apportionment from Las Vegas measurements

The analysis described in Section 3.2 provides a perspective of the key VOCs emitted from commercial cooking. Other VOCs are also likely associated with cooking but are not resolved by a simple correlation analysis due to the presence of other important sources along the Las Vegas Strip, such as ethanol from VCPs or monoterpenes from fragranced consumer products. Moreover, emissions from residential cooking may also contribute to regional VOC mixing ratios. Here, we discuss the PMF results to determine the emissions profile and the contribution of cooking to total VOC emissions observed at the Jerome Mack ground site.

Figures 8 and 9 show the PMF solution for the data collected at the Jerome Mack ground site. Figure 8 shows the time series and factor profiles, while Fig. 9 shows the average diurnal profiles. We present a 5-factor solution where VOCs are apportioned to (1) a mobile source factor, (2) a VCP-dominated factor, (3) a cooking-dominated factor, (4) a regional background plus secondary oxidation processes, and (5) a local solvent source. A full description of the PMF results is provided in the Supplemental Information.

The mobile source factor is largely composed of ethanol (EOH) and C_6-C_{10} aromatics (Fig. S8). The VCP-dominated factor is primarily composed of ethanol, but also contains D5-siloxane, monoterpenes, and acetone, which are common ingredients in consumer products. Both factors resemble the solution presented by Gkatzelis et al. (2021b) for New York City. The mobile source factor had the highest correlation to CO measured at the ground site ($R^2 = 0.72$), which is consistent with the expectation that mobile sources are important contributors to the variability of CO in urban areas (McDonald et al., 2013). The VCP-dominated factor was also correlated to CO ($R^2 = 0.67$) and likely results from the coincidental emission of VCPs and mobile sources over similar temporal and spatial scales. Similar behavior was proposed to drive correlations between VCP and mobile source emissions observed in other cities, such as New York City, Boulder, CO, and Toronto, ON (Coggon et al., 2018; Gkatzelis et al., 2021a; Gkatzelis et al., 2021b)

The VCP-dominated factor derived here has two key differences from the factor derived by Gkatzelis et al. (2021b). First, the VCP-dominated factor from New York City contained a series of other VCP markers, including parachlorobenzotriflouride (PCBTF) and D4-siloxane. These molecules are largely associated with construction activity and are expected to be emitted from the application of industrial coatings and adhesives (Gkatzelis et al., 2021a; Stockwell et al., 2021). PCBTF was attributed to the VCP-dominated factor at the Jerome Mack ground site, but was also associated with the local solvent factor which appeared to come from a point source located near the ground site (Fig. 8). Second, the VCP-dominated factor reported by Gkatzelis et al. (2021b) also contained methyl ethyl ketone, which is a prominent solvent in consumer and industrial VCPs. Methyl ethyl ketone was excluded from this analysis due to a water cluster interference produced within the Vocus drift tube.

The oxidation factor is largely composed of multiple oxygenated carbon-containing masses, which agrees with secondary factors resolved by PMF in other cities (Gkatzelis et al., 2021b; Peng et al., 2022). At the Jerome Mack site, this factor also contained VOCs that are emitted during daytime hours from biogenic sources (e.g., isoprene, monoterpenes) due to emissions from urban vegetation. In general, isoprene and monoterpenes had relatively low mixing ratios over the analyzed sampling period (< 150 ppt). For comparison, measurements in Los Angeles during RECAP-CA show that average isoprene mixing ratios exceeded 2 ppb (Coggon et al., 2024). This difference highlights that urban vegetation emissions in Las Vegas are significantly lower than other cities.

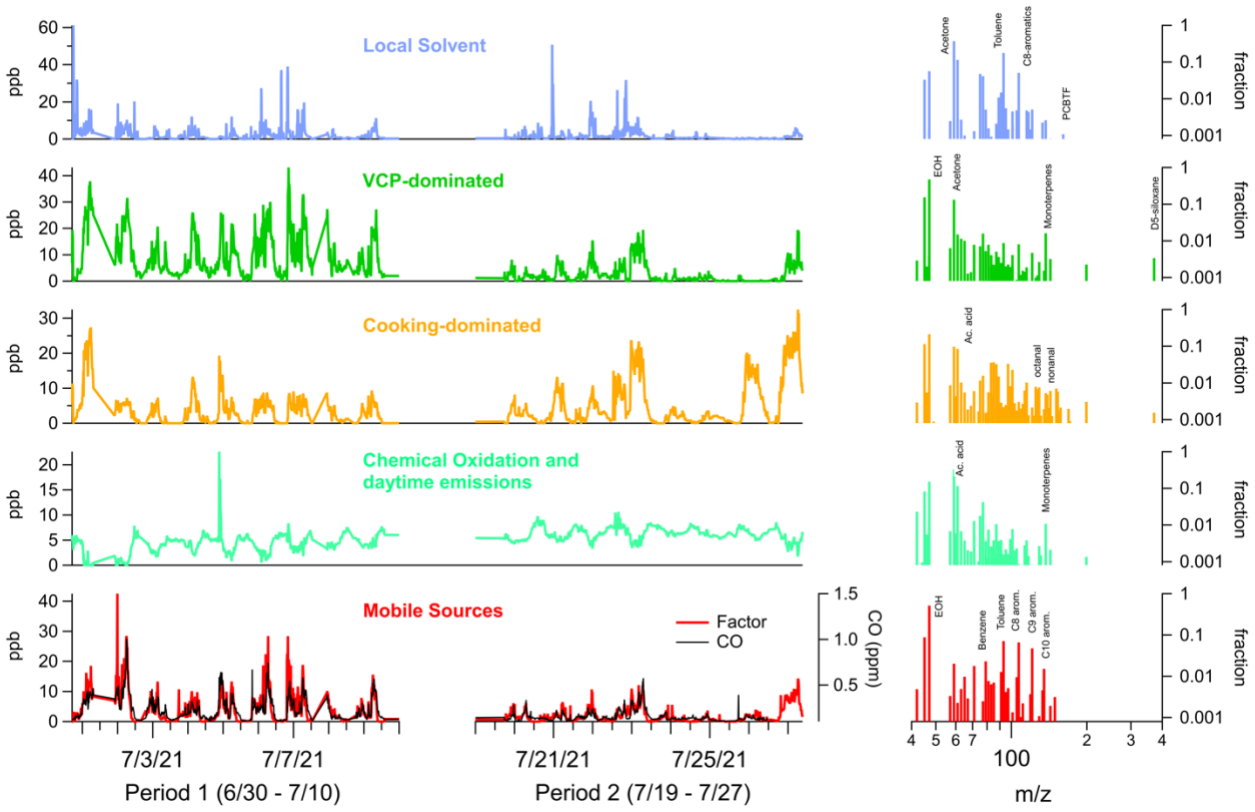

Figure 8: 5-factor PMF solution for the ground site data at Jerome Mack. Shown are the factor time profiles for the two time periods considered for this analysis (Period 1, 30 June–10 July and Period 2, 19–27 July) along with the resolved factor profiles. CO measurements are shown alongside the mobile source factor in the bottom panel.

PMF of the Jerome Mack data resolves a factor that is enriched in aldehydes, which we interpret as the cooking-dominated factor. This factor includes contributions from octanal, nonanal, acetic acid, acrolein, and higher carbon aldehydes and acids, which is consistent with the cooking emissions observed along the Las Vegas Strip and downwind of restaurants. Figure S12 compares the PMF profile to the VOC/nonanal profiles resolved by the mobile laboratory and shows that the two profiles agree for overlapping species. This agreement supports the PMF resolution of mass associated with important cooking VOCs. The PMF factor also includes ethanol, monoterpenes, and acetone/propanal, which were not resolved by the mobile laboratory analysis. Cooking emits significant amounts of ethanol and monoterpenes to indoor air (Arata et al., 2021; Klein et al., 2016a), and is a dominant source of total VOC emissions in residential indoor air (Arata et al., 2021; Klein et al., 2019). These species represent ~22% of the cooking-dominated factor.

Figure 9 shows daily mass concentrations for each factor. Gkatzelis et al. (2021b) found that ~53% of mobile source emissions and ~50% of VCP emissions are associated with molecules that cannot be resolved by PTR-ToF-MS (e.g., alkanes and small alkenes). The mobile source and

VCP-dominated factors shown in Figures 9 and 10 have been adjusted by the following equation to account for this unresolved mass.

$$M_{total} = \frac{M}{a}$$

M_{total} is the adjusted PMF factor, M is factor mass, and a is the fraction of the factor mass estimated by Gkatzelis et al. (2021b) to be measured by PTR-ToF-MS for VCP (0.5) and mobile source (0.47) emissions. No adjustments are applied to the cooking-dominated, solvent, or oxidation factor as it is assumed that PTR-ToF-MS measures the key VOCs from these sources. This may not account for mass that has been previously reported from cooking emissions, such as alkanes or alkenes (Schauer et al., 1999).

For the mobile source, VCP-dominated, and cooking-dominated factors, mass concentrations are highest at night when the nocturnal boundary layer is shallow. In the daytime, the boundary layer rapidly rises to as high as 4 km (Langford et al., 2022), and VOC concentrations decrease in response. In contrast, the chemical oxidation + daytime emissions factor increases during daytime hours, further supporting that this factor is largely driven by secondary processes.

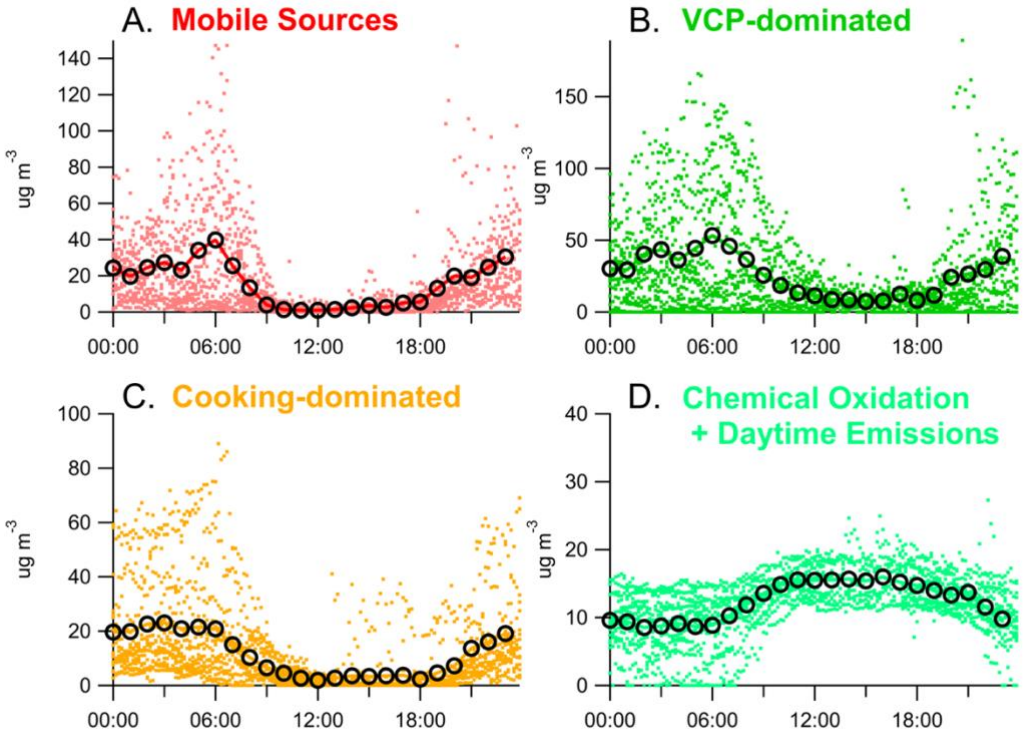

Figure 9: Diurnal patterns for the four factors resolved by PMF at the Jerome Mack ground site. The black circles show the hourly mean values calculated over the full PMF solution.

Figure 10A shows the fraction (f_i) that each primary factor contributes to total VOC mass resolved by PMF at the Jerome Mack ground site.

$$f_i = \frac{M_i}{\sum M_i}$$

Where M_i is the mass concentration of the VCP-dominated, mobile source, and cooking-dominated factors. Here, the denominator represents the total anthropogenic emissions resolved by PMF. The local solvent factor is excluded from this analysis since it is not representative of regional VOC concentrations. Figure 10B shows the average factor contribution over the entire analysis period.

Figure 10A shows that each factor contributes to the total anthropogenic emissions at different times of day depending on the emission patterns. The VCP-dominated factor is the largest contributor to total VOC emissions in Las Vegas and constitutes 40 – 80% of the primary VOCs resolved by PMF. These concentrations are largely driven by the high emissions of solvents, such as ethanol and acetone, which is consistent with observations from NYC (Gkatzelis et al., 2021b). Emissions inventories indicate that these molecules are primarily emitted from the personal care product sector (see Section 5). VCP emissions exhibit the highest relative abundances early in the day (~11:00 AM), then decrease in relative abundance throughout the day. This behavior is similar to the diurnal pattern of personal care product emissions observed in cities such as Boulder, CO where the mixing ratios of D5-siloxane from deodorants and hair products peak during morning hours and decayed as personal care products evaporate (Coggon et al., 2018). During evening and rush hour periods, mobile sources constitute ~ 30-40% of the total primary VOC mixing ratios, but then decrease during midday due to both a large enhancement of VCPs, but also lower emissions from mobile sources. Over the entire dataset, VCPs and mobile sources are estimated to represent 54% and 25% of the total anthropogenic VOCs, respectively (Fig. 10B).

The cooking-dominated factor represents 10-30% of the total primary VOC mass resolved by PMF, depending on the time of day. The relative fraction of the cooking-dominated factor peaks in the mid-afternoon, as well as in the evening and night when activity along the Las Vegas Strip is highest. Similar behavior has been observed in the relative abundance of primary cooking organic aerosol in cities such as Los Angeles (Hayes et al., 2013). The cooking-dominated factor is estimated to represent as much as 21% of the total anthropogenic VOCs over the entire dataset.

The fraction of cooking VOCs estimated here (21%) is specific to a site downwind of the Las Vegas Strip where restaurants are abundant. These impacts are likely to vary across urban areas based on ground site locations, restaurant density, and differences in the proportions of fossil fuel and VCP emissions. Cooking emissions are commonly resolved from the source apportionment of organic aerosol measurements in US cities (e.g., Hayes et al., 2013; Lyu et al., 2019; Zhang et al.,

2019; Xu et al., 2015). Far fewer studies have estimated the impact of cooking on the outdoor VOC burden in US urban areas. Recently, cooking emissions were identified from source apportionment of thermal desorption aerosol gas chromatograms and shown to be present at significant mixing ratios in Livermore, CA (Wernis et al., 2022). Similarly, source apportionment of PTR-ToF-MS data from Atlanta, GA shows that cooking emissions mixed with biomass burning were responsible for 6–15% of the reported VOC carbon, which included contributions from fossil fuel, VCPs, and biogenic sources (Peng et al., 2022). These proportions are similar to those reported here, suggesting that cooking VOCs represent a significant fraction of total anthropogenic VOCs in other US cities. Tables S1 and S2 summarizes the cooking profile resolved by the PMF analysis. This profile could be used to compare against measurements of cooking VOCs in other urban areas.

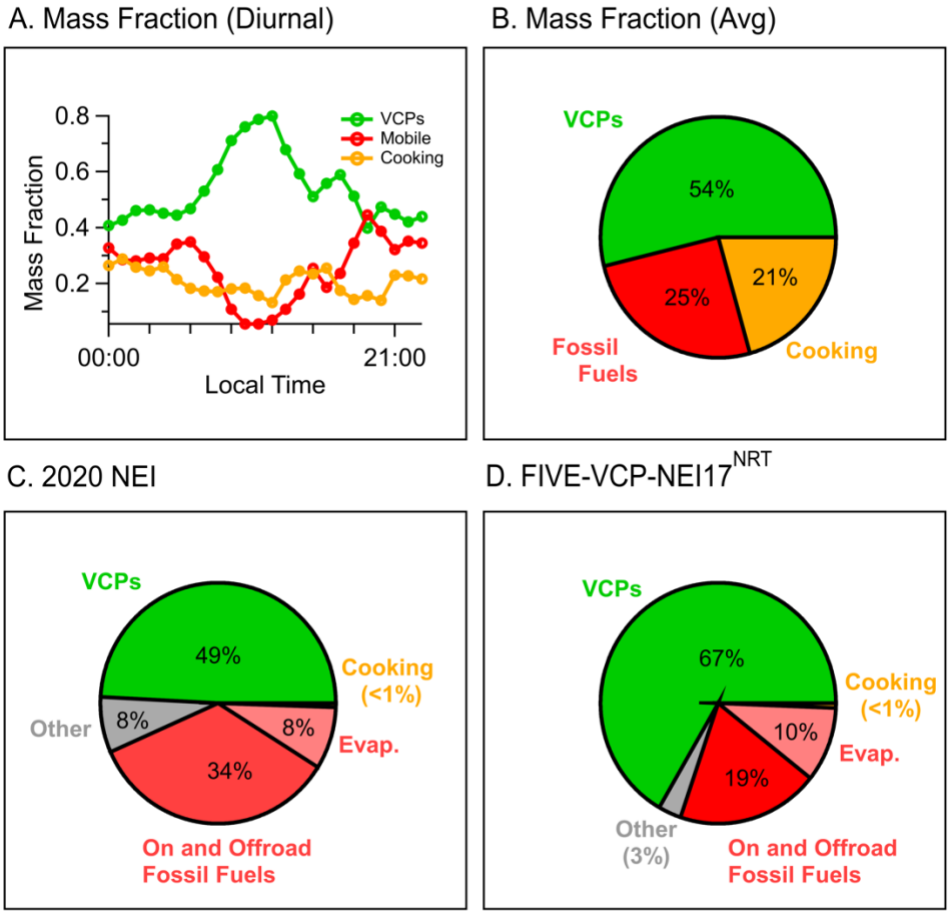

Figure 10: (A) Diurnal contribution of VCP, mobile sources, and cooking factors to the sum of primary emissions apportioned by PMF (= VCP + mobile source + cooking). (B) Average contribution of the VCP, mobile source, and mobile source factors to the PMF solution. (C) Distribution of anthropogenic VOC emissions from the 2020 National Emissions Inventory for Clark County, NV. (D) Distribution of

anthropogenic VOCs from FIVE-VCP-NEI17^{NRT} in Clark County, NV. The "other" category in both inventories reflect emissions from industry, farming, and electric power generation.

5. Comparison to Inventory Emissions

The PMF results shown in Figure 10B are compared against the distribution of anthropogenic VOCs reported in emissions inventories used to model air quality (Figure 10, panels C and D). Panel C shows emissions reported in the 2020 National Emissions Inventory (NEI) for Clark County, NV. The NEI is a benchmark for determining US emissions standards and its methodology is fully described by the US Environmental Protection Agency (EPA, 2023). The NEI for Clark County includes emissions for mobile sources (e.g., on- and offroad vehicles), fossil fuel evaporative sources (e.g., gasoline stations), solvent evaporative sources (e.g., VCPs), and miscellaneous point and area sources. Cooking emissions in the NEI predominantly result from commercial sources with minor contributions from residential backyard barbequing.

Panel D shows the distribution of VOCs represented by the FIVE-VCP-NEI17^{NRT} inventory described by He et al. (2023). The FIVE-VCP inventory was developed following the methods prescribed by McDonald et al. (2018) and was recently used to determine VCP impacts on air quality in US cities (e.g., Coggon et al., 2021; Qin et al., 2021). He et al. (2023) updated FIVE-VCP to include 2017 NEI emissions (NEI17) and revised VOC emissions with near real-time (NRT) adjustment factors to account for COVID-19 impacts on various emission sectors. Mobile source emissions are determined from fuel sales and on-road and off-road emission factors. VCP emissions are estimated based on the mass balance of the chemical product industry for 2010 then adjusted to 2021 emissions based on the long-term declining trends in VCP emissions reported by Kim et al. (2022) and economic scaling factors reported by He et al. (2023). Other sectors are from the NEI17 and are similarly updated with near real-time adjustment factors. Cooking emissions in FIVE-VCP-NEI17^{NRT} are the same as those used in the 2017 NEI.

The 2020 NEI and FIVE-VCP-NEI17^{NRT} inventories both indicate that VCPs are the dominant VOC emission sources in Clark County. Fossil fuel emissions are the next largest source, though differences between the two inventories are evident. In the NEI, total fossil fuel emissions (= on- and offroad emissions + evaporative emissions) are 15% lower than VCP emissions. In FIVE-VCP-NEI17^{NRT}, fossil fuel emissions are 57% lower than VCPs. These differences are reflected in previous comparisons between the NEI and FIVE-VCP (Coggon et al., 2021; McDonald et al., 2018). The PMF solution shows that fossil fuels are ~54% lower than VCPs, which is most consistent with FIVE-VCP-NEI17^{NRT}. Zhu et al. (2023) show that FIVE-VCP speciation agrees well with VOCs primarily emitted from fossil fuel and VCPs reported during SUNVEx and RECAP-CA. Aldehydes, ethanol, and monoterpenes were underestimated which may point to the importance of missing emission sources, such as cooking.

The fraction of total cooking VOC emissions represented in both inventories is significantly lower than the fraction resolved by PMF. Commercial sources dominate the cooking emissions in the 2017 and 2020 NEI and are estimated based on food consumption estimates and emission factors derived from laboratory studies (e.g., Schauer et al., 1999). The differences between the PMF results and what is reported in the inventories may be partially explained by the spatial scale of the datasets – the inventories represent county-level emissions estimates, while the observations are specific to a site strongly influenced by the Las Vegas Strip. Restaurant statistics indicate that the Strip and downtown regions of Las Vegas have ~550 restaurants (Fig. 1). In July 2021, approximately 106,000 tourists visited Las Vegas every day (LVCVA, 2024). Assuming that the tourism population dominates in this region, this would suggest that there are ~530 restaurants per 100,000 people within the entertainment districts. In contrast, there are ~5000 restaurants and 2.4 million (including tourists) in Clark County, which equates to ~210 restaurants per 100,000 people county-wide. This suggests that the ratio of cooking / VCP emissions along the Las Vegas Strip may be more than twice as high as those in Clark County. These differences do not account for other factors that may affect emissions, such as the types of cooking conducted in each region.

Despite the potential variability in emission patterns between datasets, Figure 10 shows that there is a significant disconnect between the cooking emissions resolved by PMF and those represented by inventories. These differences highlight the need for further analysis. It is possible that the emission factors and/or consumption of oils, meats, and other foods are different from what is reflected in laboratory studies.

6. Conclusions

Mobile laboratory and ground site measurements were analyzed to determine the importance of cooking emissions on urban VOC composition in Las Vegas, NV. PTR-ToF-MS data show that cooking is a significant source of long-chain aldehydes to urban air. Measurements of octanal and nonanal are found to be useful markers to evaluate cooking emissions due to their abundance in restaurant plumes and local enhancements in areas with high restaurant density. A comparison of the mass spectra downwind of restaurants to those obtained in regions with significant commercial cooking show similar distributions in aldehydes and fatty acids known to be emitted from laboratory cooking experiments.

Based on a PMF analysis, it is estimated that cooking emissions represent as much as 20% of the anthropogenic VOCs emitted to the atmosphere in Las Vegas, NV. It is expected that the relative importance of cooking emissions in other cities will vary based on regional restaurant density and the magnitude of other anthropogenic emissions including VCPs and mobile sources. More work is needed to quantify cooking in other urban areas. Measurements from this study in Pasadena, CA (Fig S12) and those conducted previously in Livermore, CA and Atlanta, GA show

that long-chain aldehydes are ubiquitous in urban air (~100 – 200 ppt) and modulated by commercial and residential cooking (Wernis et al., 2022; Peng et al., 2022). The source apportionment profiles determined here may be compared against other urban environments to evaluate cooking in other cities.

The VOCs emitted from cooking are reactive and may contribute to the formation of ozone, secondary organic aerosol, and other pollutants such as peroxyacyl nitrates (Bowman et al., 2003). A review of VOC emissions inventories show that total cooking emissions (i.e., residential + commercial cooking) are likely underrepresented in air quality models. Spatial patterns of long-chain aldehydes suggest that more work is needed to quantify the magnitude of emissions from commercial cooking, which are also important sources of primary urban SOA (Robinson et al., 2018; Shah et al., 2018). PMF results in Las Vegas suggest that cooking emissions may be as important to urban VOCs as mobile sources in regions with significant restaurant activity.

Data Availability

Data for SUNVEx and RE-CAP are available at the NOAA CSL data repository (https://csl.noaa.gov/projects/sunvex/).

Author Contribution

MMC, CES, XL, JBG, AL, JP, HJB, KA, and CW conducted measurements during SUNVEx and RE-CAP. CH, QZ, RHS, JH, ML, KS, and BC developed inventories used to compare against observations. MMC and CW wrote the paper with contributions from all authors.

Competing Interests

The authors also have no other competing interests to declare.

Acknowledgements

MMC, CES, QZ, and RHS acknowledge support from the U.S. Environmental Protection Agency (EPA) STAR program (grant # 84001001). The views expressed in this document are solely those of the authors and do not necessarily reflect those of the Agency. EPA does not endorse any products or commercial services mentioned in this publication. CW, MMC, CES, LX, JBG, and AL acknowledge measurement funding from Clark County, NV (contract number 20-022001) and the California Air Resources Board (contract number 20RD002). This work was supported in part by the NOAA Cooperative Agreements with CIRES, NA17OAR4320101 and NA22OAR4320151. The authors thank Paul Wennberg, John Seinfeld, and Ben Schulze for their coordination of the Caltech ground site during RECAP-CA.

References

730
731 Arata, C., Misztal, P. K., Tian, Y., Lunderberg, D. M., Kristensen, K., Novoselac, A., Vance, M. E.,
732 Farmer, D. K., Nazaroff, W. W., and Goldstein, A. H.: Volatile organic compound emissions
733 during HOMEChem, Indoor Air, 31, 2099-2117, https://doi.org/10.1111/ina.12906, 2021.

734 Bastos, L. C., and Pereira, P. A.: Influence of heating time and metal ions on the amount of free
735 fatty acids and formation rates of selected carbonyl compounds during the thermal oxidation of
736 canola oil, J Agric Food Chem, 58, 12777-12783, 10.1021/jf1028575, 2010.

737 Bowman, J. H., Barket, D. J., and Shepson, P. B.: Atmospheric Chemistry of Nonanal,
738 Environmental Science & Technology, 37, 2218-2225, 10.1021/es026220p, 2003.

739 Canonaco, F., Crippa, M., Slowik, J. G., Baltensperger, U., and Prévôt, A. S. H.: SoFi, an IGOR-
740 based interface for the efficient use of the generalized multilinear engine (ME-2) for the source
741 apportionment: ME-2 application to aerosol mass spectrometer data, Atmos. Meas. Tech., 6,
742 3649-3661, 10.5194/amt-6-3649-2013, 2013.

743 Churkina, G., Kuik, F., Bonn, B., Lauer, A., Grote, R., Tomiak, K., and Butler, T. M.: Effect of VOC
744 Emissions from Vegetation on Air Quality in Berlin during a Heatwave, Environmental Science &
745 Technology, 51, 6120-6130, 10.1021/acs.est.6b06514, 2017.

746 Coggon, M. M., Veres, P. R., Yuan, B., Koss, A., Warneke, C., Gilman, J. B., Lerner, B. M., Peischl,
747 J., Aikin, K. C., Stockwell, C. E., Hatch, L. E., Ryerson, T. B., Roberts, J. M., Yokelson, R. J., and de
748 Gouw, J. A.: Emissions of nitrogen-containing organic compounds from the burning of
749 herbaceous and arboraceous biomass: Fuel composition dependence and the variability of
750 commonly used nitrile tracers, Geophys. Res. Lett., 43, 9903-9912, 10.1002/2016gl070562,
751 2016.

752 Coggon, M. M., McDonald, B. C., Vlasenko, A., Veres, P. R., Bernard, F., Koss, A. R., Yuan, B.,
753 Gilman, J. B., Peischl, J., Aikin, K. C., DuRant, J., Warneke, C., Li, S. M., and de Gouw, J. A.:
754 Diurnal Variability and Emission Pattern of Decamethylcyclopentasiloxane (D5) from the
755 Application of Personal Care Products in Two North American Cities, Environ. Sci. Technol., 52,
756 5610-5618, 10.1021/acs.est.8b00506, 2018.

757 Coggon, M. M., Gkatzelis, G. I., McDonald, B. C., Gilman, J. B., Schwantes, R. H., Abuhassan, N.,
758 Aikin, K. C., Arend, M. F., Berkoff, T. A., Brown, S. S., Campos, T. L., Dickerson, R. R., Gronoff, G.,
759 Hurley, J. F., Isaacman-VanWertz, G., Koss, A. R., Li, M., McKeen, S. A., Moshary, F., Peischl, J.,
760 Pospisilova, V., Ren, X., Wilson, A., Wu, Y., Trainer, M., and Warneke, C.: Volatile chemical
761 product emissions enhance ozone and modulate urban chemistry, Proceedings of the National
762 Academy of Sciences, 118, e2026653118, doi:10.1073/pnas.2026653118, 2021.

763 Coggon, M. M., Stockwell, C. E., Claflin, M. S., Pfannerstill, E. Y., Xu, L., Gilman, J. B.,
764 Marcantonio, J., Cao, C., Bates, K., Gkatzelis, G. I., Lamplugh, A., Katz, E. F., Arata, C., Apel, E. C.,
765 Hornbrook, R. S., Piel, F., Majluf, F., Blake, D. R., Wisthaler, A., Canagaratna, M., Lerner, B. M.,
766 Goldstein, A. H., Mak, J. E., and Warneke, C.: Identifying and correcting interferences to PTR-

ToF-MS measurements of isoprene and other urban volatile organic compounds, Atmos. Meas. Tech., 17, 801-825, 10.5194/amt-17-801-2024, 2024.

de Gouw, J. A., Gilman, J. B., Kim, S.-W., Alvarez, S. L., Dusanter, S., Graus, M., Griffith, S. M., Isaacman-VanWertz, G., Kuster, W. C., Lefer, B. L., Lerner, B. M., McDonald, B. C., Rappenglück, B., Roberts, J. M., Stevens, P. S., Stutz, J., Thalman, R., Veres, P. R., Volkamer, R., Warneke, C., Washenfelder, R. A., and Young, C. J.: Chemistry of Volatile Organic Compounds in the Los Angeles Basin: Formation of Oxygenated Compounds and Determination of Emission Ratios, Journal of Geophysical Research: Atmospheres, 123, 2298-2319, https://doi.org/10.1002/2017JD027976, 2018.

Eilerman, S. J., Peischl, J., Neuman, J. A., Ryerson, T. B., Aikin, K. C., Holloway, M. W., Zondlo, M. A., Golston, L. M., Pan, D., Floerchinger, C., and Herndon, S.: Characterization of Ammonia, Methane, and Nitrous Oxide Emissions from Concentrated Animal Feeding Operations in Northeastern Colorado, Environmental Science & Technology, 50, 10885-10893, 10.1021/acs.est.6b02851, 2016.

US Environmental Protection Agency: 2020 National Emissions Inventory (NEI): https://www.epa.gov/air-emissions-inventories/2020-national-emissions-inventory-nei-data, 2023.

Gentner, D. R., Worton, D. R., Isaacman, G., Davis, L. C., Dallmann, T. R., Wood, E. C., Herndon, S. C., Goldstein, A. H., and Harley, R. A.: Chemical composition of gas-phase organic carbon emissions from motor vehicles and implications for ozone production, Environ. Sci. Technol., 47, 11837-11848, 10.1021/es401470e, 2013.

Gkatzelis, G. I., Coggon, M. M., McDonald, B. C., Peischl, J., Aikin, K. C., Gilman, J. B., Trainer, M., and Warneke, C.: Identifying Volatile Chemical Product Tracer Compounds in U.S. Cities, Environmental Science & Technology, 55, 188-199, 10.1021/acs.est.0c05467, 2021a.

Gkatzelis, G. I., Coggon, M. M., McDonald, B. C., Peischl, J., Gilman, J. B., Aikin, K. C., Robinson, M. A., Canonaco, F., Prevot, A. S. H., Trainer, M., and Warneke, C.: Observations Confirm that Volatile Chemical Products Are a Major Source of Petrochemical Emissions in U.S. Cities, Environmental Science & Technology, 55, 4332-4343, 10.1021/acs.est.0c05471, 2021b.

Gueneron, M., Erickson, M. H., VanderSchelden, G. S., and Jobson, B. T.: PTR-MS fragmentation patterns of gasoline hydrocarbons, International Journal of Mass Spectrometry, 379, 97-109, https://doi.org/10.1016/j.ijms.2015.01.001, 2015.

Hayes, P. L., Ortega, A. M., Cubison, M. J., Froyd, K. D., Zhao, Y., Cliff, S. S., Hu, W. W., Toohey, D. W., Flynn, J. H., Lefer, B. L., Grossberg, N., Alvarez, S., Rappenglück, B., Taylor, J. W., Allan, J. D., Holloway, J. S., Gilman, J. B., Kuster, W. C., de Gouw, J. A., Massoli, P., Zhang, X., Liu, J., Weber, R. J., Corrigan, A. L., Russell, L. M., Isaacman, G., Worton, D. R., Kreisberg, N. M., Goldstein, A. H., Thalman, R., Waxman, E. M., Volkamer, R., Lin, Y. H., Surratt, J. D., Kleindienst, T. E., Offenberg, J. H., Dusanter, S., Griffith, S., Stevens, P. S., Brioude, J., Angevine, W. M., and

804 Jimenez, J. L.: Organic aerosol composition and sources in Pasadena, California, during the 2010
805 CalNex campaign, Journal of Geophysical Research: Atmospheres, 118, 9233-9257,
806 10.1002/jgrd.50530, 2013.

807 He, J., Harkins, C., O'Dell, K., Li, M., Francoeur, C., Anenberg, S., Brown, S. S., Coggon, M. M.,
808 Frost, G. J., Gilman, J. B., Kongdragunta, S., Lamplugh, A., Pierce, B., Schwantes, R. H., Stockwell,
809 C. E., Warneke, C., Yang, K., and McDonald, B. C.: COVID-19 perturbation on US air quality and
810 human health impact assessment, in review., 2023.

811 Hurley, J. F., Smiley, E., and Isaacman-VanWertz, G.: Modeled Emission of Hydroxyl and Ozone
812 Reactivity from Evaporation of Fragrance Mixtures, Environmental Science & Technology, 55,
813 15672-15679, 10.1021/acs.est.1c04004, 2021.

814 Karl, T., Striednig, M., Graus, M., Hammerle, A., and Wohlfahrt, G.: Urban flux measurements
815 reveal a large pool of oxygenated volatile organic compound emissions, Proc. Natl. Acad. Sci.
816 U.S.A., 115, 1186-1191, 10.1073/pnas.1714715115, 2018.

817 Kilgour, D., Novak, G., and Bertram, T.: Observations of Biotic and Abiotic Marine Volatile
818 Organic Compounds Emitted from Coastal Seawater, December 01, 2021, 2021.

819 Kim, S.-W., McDonald, B. C., Seo, S., Kim, K.-M., and Trainer, M.: Understanding the Paths of
820 Surface Ozone Abatement in the Los Angeles Basin, Journal of Geophysical Research:
821 Atmospheres, 127, e2021JD035606, https://doi.org/10.1029/2021JD035606, 2022.

822 Klein, F., Farren, N. J., Bozzetti, C., Daellenbach, K. R., Kilic, D., Kumar, N. K., Pieber, S. M.,
823 Slowik, J. G., Tuthill, R. N., Hamilton, J. F., Baltensperger, U., Prevot, A. S., and El Haddad, I.:
824 Indoor terpene emissions from cooking with herbs and pepper and their secondary organic
825 aerosol production potential, Sci. Rep., 6, 36623, 10.1038/srep36623, 2016a.

826 Klein, F., Platt, S. M., Farren, N. J., Detournay, A., Bruns, E. A., Bozzetti, C., Daellenbach, K. R.,
827 Kilic, D., Kumar, N. K., Pieber, S. M., Slowik, J. G., Temime-Roussel, B., Marchand, N., Hamilton,
828 J. F., Baltensperger, U., Prévôt, A. S. H., and El Haddad, I.: Characterization of Gas-Phase
829 Organics Using Proton Transfer Reaction Time-of-Flight Mass Spectrometry: Cooking Emissions,
830 Environmental Science & Technology, 50, 1243-1250, 10.1021/acs.est.5b04618, 2016b.

831 Klein, F., Baltensperger, U., Prévôt, A. S. H., and El Haddad, I.: Quantification of the impact of
832 cooking processes on indoor concentrations of volatile organic species and primary and
833 secondary organic aerosols, Indoor Air, 29, 926-942, https://doi.org/10.1111/ina.12597, 2019.

834 Koss, A. R., Sekimoto, K., Gilman, J. B., Selimovic, V., Coggon, M. M., Zarzana, K. J., Yuan, B.,
835 Lerner, B. M., Brown, S. S., Jimenez, J. L., Krechmer, J., Roberts, J. M., Warneke, C., Yokelson, R.
836 J., and de Gouw, J.: Non-methane organic gas emissions from biomass burning: identification,
837 quantification, and emission factors from PTR-ToF during the FIREX 2016 laboratory
838 experiment, Atmos. Chem. Phys., 18, 3299-3319, 10.5194/acp-18-3299-2018, 2018.

839 Krechmer, J., Lopez-Hilfiker, F., Koss, A., Hutterli, M., Stoermer, C., Deming, B., Kimmel, J.,
840 Warneke, C., Holzinger, R., Jayne, J., Worsnop, D., Fuhrer, K., Gonin, M., and de Gouw, J.:
841 Evaluation of a New Reagent-Ion Source and Focusing Ion–Molecule Reactor for Use in Proton-
842 Transfer-Reaction Mass Spectrometry, Analytical Chemistry, 90, 12011-12018,
843 10.1021/acs.analchem.8b02641, 2018.

844 Kruza, M., Lewis, A. C., Morrison, G. C., and Carslaw, N.: Impact of surface ozone interactions on
845 indoor air chemistry: A modeling study, Indoor Air, 27, 1001-1011,
846 https://doi.org/10.1111/ina.12381, 2017.

847 Langford, A. O., Senff, C. J., Alvarez Ii, R. J., Aikin, K. C., Baidar, S., Bonin, T. A., Brewer, W. A.,
848 Brioude, J., Brown, S. S., Burley, J. D., Caputi, D. J., Conley, S. A., Cullis, P. D., Decker, Z. C. J.,
849 Evan, S., Kirgis, G., Lin, M., Pagowski, M., Peischl, J., Petropavlovskikh, I., Pierce, R. B., Ryerson,
850 T. B., Sandberg, S. P., Sterling, C. W., Weickmann, A. M., and Zhang, L.: The Fires, Asian, and
851 Stratospheric Transport–Las Vegas Ozone Study (FAST-LVOS), Atmos. Chem. Phys., 22, 1707-
852 1737, 10.5194/acp-22-1707-2022, 2022.

853 Liu, Y., Misztal, P. K., Arata, C., Weschler, C. J., Nazaroff, W. W., and Goldstein, A. H.: Observing
854 ozone chemistry in an occupied residence, Proceedings of the National Academy of Sciences,
855 118, e2018140118, doi:10.1073/pnas.2018140118, 2021.

856 Las Vegas Convention and Visitors Authority (LVCVA) Executive Summary of Sourthern Nevada
857 Tourism Indicators: https://www.lvcva.com/research/visitor-statistics/, access: February 22,
858 2024, 2024.

859 Lyu, R., Alam, M. S., Stark, C., Xu, R., Shi, Z., Feng, Y., and Harrison, R. M.: Aliphatic carbonyl
860 compounds (C8–C26) in wintertime atmospheric aerosol in London, UK, Atmos. Chem. Phys.,
861 19, 2233-2246, 10.5194/acp-19-2233-2019, 2019.

862 McDonald, B. C., Gentner, D. R., Goldstein, A. H., and Harley, R. A.: Long-term trends in motor
863 vehicle emissions in u.s. urban areas, Environ. Sci. Technol., 47, 10022-10031,
864 10.1021/es401034z, 2013.

865 McDonald, B. C., de Gouw, J. A., Gilman, J. B., Jathar, S. H., Akherati, A., Cappa, C. D., Jimenez, J.
866 L., Lee-Taylor, J., Hayes, P. L., McKeen, S. A., Cui, Y. Y., Kim, S. W., Gentner, D. R., Isaacman-
867 VanWertz, G., Goldstein, A. H., Harley, R. A., Frost, G. J., Roberts, J. M., Ryerson, T. B., and
868 Trainer, M.: Volatile chemical products emerging as largest petrochemical source of urban
869 organic emissions, Science, 359, 760-764, 10.1126/science.aaq0524, 2018.

870 McDonald, J. D., Zielinska, B., Fujita, E. M., Sagebiel, J. C., Chow, J. C., and Watson, J. G.: Fine
871 Particle and Gaseous Emission Rates from Residential Wood Combustion, Environmental
872 Science & Technology, 34, 2080-2091, 10.1021/es9909632, 2000.

Peng, C. Y., Lan, C. H., Lin, P. C., and Kuo, Y. C.: Effects of cooking method, cooking oil, and food type on aldehyde emissions in cooking oil fumes, J Hazard Mater, 324, 160-167, 10.1016/j.jhazmat.2016.10.045, 2017.

Peng, Y., Mouat, A. P., Hu, Y., Li, M., McDonald, B. C., and Kaiser, J.: Source appointment of volatile organic compounds and evaluation of anthropogenic monoterpene emission estimates in Atlanta, Georgia, Atmospheric Environment, 288, 119324, https://doi.org/10.1016/j.atmosenv.2022.119324, 2022.

Pye, H. O. T., Place, B. K., Murphy, B. N., Seltzer, K. M., D'Ambro, E. L., Allen, C., Piletic, I. R., Farrell, S., Schwantes, R. H., Coggon, M. M., Saunders, E., Xu, L., Sarwar, G., Hutzell, W. T., Foley, K. M., Pouliot, G., Bash, J., and Stockwell, W. R.: Linking gas, particulate, and toxic endpoints to air emissions in the Community Regional Atmospheric Chemistry Multiphase Mechanism (CRACMM), Atmos. Chem. Phys., 23, 5043-5099, 10.5194/acp-23-5043-2023, 2023.

Qin, M., Murphy, B. N., Isaacs, K. K., McDonald, B. C., Lu, Q., McKeen, S. A., Koval, L., Robinson, A. L., Efstathiou, C., Allen, C., and Pye, H. O. T.: Criteria pollutant impacts of volatile chemical products informed by near-field modelling, Nature Sustainability, 4, 129-137, 10.1038/s41893-020-00614-1, 2021.

Roberts, J. M., Neuman, J. A., Brown, S. S., Veres, P. R., Coggon, M. M., Stockwell, C. E., Warneke, C., Peischl, J., and Robinson, M. A.: Furoyl peroxynitrate (fur-PAN), a product of VOC–NOx photochemistry from biomass burning emissions: photochemical synthesis, calibration, chemical characterization, and first atmospheric observations, Environmental Science: Atmospheres, 2, 1087-1100, 10.1039/D2EA00068G, 2022.

Robinson, A. L., Subramanian, R., Donahue, N. M., Bernardo-Bricker, A., and Rogge, W. F.: Source Apportionment of Molecular Markers and Organic Aerosol. 3. Food Cooking Emissions, Environmental Science & Technology, 40, 7820-7827, 10.1021/es060781p, 2006.

Robinson, E. S., Gu, P., Ye, Q., Li, H. Z., Shah, R. U., Apte, J. S., Robinson, A. L., and Presto, A. A.: Restaurant Impacts on Outdoor Air Quality: Elevated Organic Aerosol Mass from Restaurant Cooking with Neighborhood-Scale Plume Extents, Environmental Science & Technology, 52, 9285-9294, 10.1021/acs.est.8b02654, 2018.

Ryerson, T. B., Andrews, A. E., Angevine, W. M., Bates, T. S., Brock, C. A., Cairns, B., Cohen, R. C., Cooper, O. R., de Gouw, J. A., Fehsenfeld, F. C., Ferrare, R. A., Fischer, M. L., Flagan, R. C., Goldstein, A. H., Hair, J. W., Hardesty, R. M., Hostetler, C. A., Jimenez, J. L., Langford, A. O., McCauley, E., McKeen, S. A., Molina, L. T., Nenes, A., Oltmans, S. J., Parrish, D. D., Pederson, J. R., Pierce, R. B., Prather, K., Quinn, P. K., Seinfeld, J. H., Senff, C. J., Sorooshian, A., Stutz, J., Surratt, J. D., Trainer, M., Volkamer, R., Williams, E. J., and Wofsy, S. C.: The 2010 California Research at the Nexus of Air Quality and Climate Change (CalNex) field study, Journal of Geophysical Research: Atmospheres, 118, 5830-5866, https://doi.org/10.1002/jgrd.50331, 2013.

Schauer, J. J., Kleeman, M. J., Cass, G. R., and Simoneit, B. R. T.: Measurement of Emissions from Air Pollution Sources. 1. C1 through C29 Organic Compounds from Meat Charbroiling, Environmental Science & Technology, 33, 1566-1577, 10.1021/es980076j, 1999.

Sekimoto, K., Li, S.-M., Yuan, B., Koss, A., Coggon, M., Warneke, C., and de Gouw, J.: Calculation of the sensitivity of proton-transfer-reaction mass spectrometry (PTR-MS) for organic trace gases using molecular properties, International Journal of Mass Spectrometry, 421, 71-94, https://doi.org/10.1016/j.ijms.2017.04.006, 2017.

Shah, R. U., Robinson, E. S., Gu, P., Robinson, A. L., Apte, J. S., and Presto, A. A.: High-spatial-resolution mapping and source apportionment of aerosol composition in Oakland, California, using mobile aerosol mass spectrometry, Atmos. Chem. Phys., 18, 16325-16344, 10.5194/acp-18-16325-2018, 2018.

Slowik, J. G., Vlasenko, A., McGuire, M., Evans, G. J., and Abbatt, J. P. D.: Simultaneous factor analysis of organic particle and gas mass spectra: AMS and PTR-MS measurements at an urban site, Atmos. Chem. Phys., 10, 1969-1988, 10.5194/acp-10-1969-2010, 2010.

Restaurant Inspections from the Southern Nevada Health District (SNHD). https://opendataportal-lasvegas.opendata.arcgis.com/datasets/restaurant-inspections-open-data/explore, access: December 28, 2021, 2021.

Stark, H., Yatavelli, R. L. N., Thompson, S. L., Kimmel, J. R., Cubison, M. J., Chhabra, P. S., Canagaratna, M. R., Jayne, J. T., Worsnop, D. R., and Jimenez, J. L.: Methods to extract molecular and bulk chemical information from series of complex mass spectra with limited mass resolution, International Journal of Mass Spectrometry, 389, 26-38, https://doi.org/10.1016/j.ijms.2015.08.011, 2015.

Steinemann, A.: Volatile emissions from common consumer products, Air Qual. Atmos. Hlth., 8, 273-281, 10.1007/s11869-015-0327-6, 2015.

Steinemann, A. C., MacGregor, I. C., Gordon, S. M., Gallagher, L. G., Davis, A. L., Ribeiro, D. S., and Wallace, L. A.: Fragranced consumer products: Chemicals emitted, ingredients unlisted, Environ. Impact. Asses., 31, 328-333, 10.1016/j.eiar.2010.08.002, 2011.

Stockwell, C. E., Coggon, M. M., Gkatzelis, G. I., Ortega, J., McDonald, B. C., Peischl, J., Aikin, K., Gilman, J. B., Trainer, M., and Warneke, C.: Volatile organic compound emissions from solvent- and water-borne coatings – compositional differences and tracer compound identifications, Atmos. Chem. Phys., 21, 6005-6022, 10.5194/acp-21-6005-2021, 2021.

Umano, K., and Shibamoto, T.: Analysis of acrolein from heated cooking oils and beef fat, Journal of Agricultural and Food Chemistry, 35, 909-912, 10.1021/jf00078a014, 1987.

Wang, N., Ernle, L., Bekö, G., Wargocki, P., and Williams, J.: Emission Rates of Volatile Organic Compounds from Humans, Environmental Science & Technology, 56, 4838-4848, 10.1021/acs.est.1c08764, 2022.

946 Warneke, C., de Gouw, J. A., Holloway, J. S., Peischl, J., Ryerson, T. B., Atlas, E., Blake, D.,
947 Trainer, M., and Parrish, D. D.: Multiyear trends in volatile organic compounds in Los Angeles,
948 California: Five decades of decreasing emissions, J. Geophs. Res., 117, 1-10,
949 10.1029/2012jd017899, 2012.

950 Wernis, R. A., Kreisberg, N. M., Weber, R. J., Drozd, G. T., and Goldstein, A. H.: Source
951 apportionment of VOCs, IVOCs and SVOCs by positive matrix factorization in suburban
952 Livermore, California, Atmos. Chem. Phys., 22, 14987-15019, 10.5194/acp-22-14987-2022,
953 2022.

954 Xu, L., Suresh, S., Guo, H., Weber, R. J., and Ng, N. L.: Aerosol characterization over the
955 southeastern United States using high-resolution aerosol mass spectrometry: spatial and
956 seasonal variation of aerosol composition and sources with a focus on organic nitrates, Atmos.
957 Chem. Phys., 15, 7307-7336, 10.5194/acp-15-7307-2015, 2015.

958 Yeoman, A. M., Shaw, M., Carslaw, N., Murrells, T., Passant, N., and Lewis, A. C.: Simplified
959 speciation and atmospheric volatile organic compound emission rates from non-aerosol
960 personal care products, Indoor Air, 30, 459-472, https://doi.org/10.1111/ina.12652, 2020.

961 Yuan, B., Koss, A., Warneke, C., Gilman, J. B., Lerner, B. M., Stark, H., and de Gouw, J. A.: A high-
962 resolution time-of-flight chemical ionization mass spectrometer utilizing hydronium ions (H3O+
963 ToF-CIMS) for measurements of volatile organic compounds in the atmosphere, Atmos. Meas.
964 Tech., 9, 2735-2752, 10.5194/amt-9-2735-2016, 2016.

965 Zhang, R., Lei, W., Tie, X., and Hess, P.: Industrial emissions cause extreme urban ozone diurnal
966 variability, Proceedings of the National Academy of Sciences, 101, 6346-6350,
967 doi:10.1073/pnas.0401484101, 2004.

968 Zhang, Y., Favez, O., Petit, J. E., Canonaco, F., Truong, F., Bonnaire, N., Crenn, V., Amodeo, T.,
969 Prévôt, A. S. H., Sciare, J., Gros, V., and Albinet, A.: Six-year source apportionment of submicron
970 organic aerosols from near-continuous highly time-resolved measurements at SIRTA (Paris area,
971 France), Atmos. Chem. Phys., 19, 14755-14776, 10.5194/acp-19-14755-2019, 2019.

972 Zhao, Y., and Zhao, B.: Emissions of air pollutants from Chinese cooking: A literature review,
973 Building Simulation, 11, 10.1007/s12273-018-0456-6, 2018.

974 Zhu, Q., Schwantes, R. H., Coggon, M. M., Harkins, C., Schnell, J., He, J., Pye, H. O. T., Li, M.,
975 Baker, B., Moon, Z., Ahmadov, R., Pfannerstill, E. Y., Place, B. K., Wooldridge, P., Schulze, B. C.,
976 Arata, C., Bucholtz, A., Seinfeld, J. H., Warneke, C., Stockwell, C. E., Xu, L., Zuraski, K., Robinson,
977 M. A., Neuman, J. A., Veres, P. R., Peischl, J., Brown, S. S., Goldstein, A. H., Cohen, R. C., and
978 McDonald, B. C.: A better representation of VOC chemistry and ozone over Los Angeles using
979 WRF-Chem, In prepration, 2023.
980